

Article

Unfolded Lipase at Interfaces Studied via Interfacial Dilational Rheology: The Impact of Urea

Saeid Dowlati ^{1,*}, Aliyar Javadi ^{2,3}, Reinhard Miller ⁴, Kerstin Eckert ^{3,5} and Matthias Kraume ¹¹ Chemical and Process Engineering, Technical University of Berlin, Ackerstraße 76, D-13355 Berlin, Germany² Institute of Radiopharmaceutical Cancer Research, Helmholtz-Zentrum Dresden-Rossendorf (HZDR), Bautzner Landstraße 400, D-01328 Dresden, Germany³ Institute of Process Engineering and Environmental Technology, Technical University of Dresden, D-01069 Dresden, Germany⁴ Department of Soft Matter Biophysics, Technical University of Darmstadt, Hochschulstraße 12, D-64289 Darmstadt, Germany⁵ Institute of Fluid Dynamics, Helmholtz-Zentrum Dresden-Rossendorf (HZDR), Bautzner Landstraße 400, D-01328 Dresden, Germany

* Correspondence: dowlati@campus.tu-berlin.de; Tel.: +49-(0)30-314-23973

Abstract: Unfolding can interrupt the activity of enzymes. Lipase, the enzyme responsible for triglyceride catalysis, can be deactivated by unfolding, which can significantly affect the yield of enzymatic processes in biochemical engineering. Different agents can induce lipase unfolding, among which we study the impact of urea as a strong denaturant. Unfolding weakens the rigidity and stability of globular proteins, thereby changing the viscoelastic properties of the protein adsorbed layers. These changes can be detected and quantified using interfacial dilational rheology. The urea-induced unfolding of lipase destructs its globular structure, making it more flexible. The interfacial tension and viscoelastic moduli of lipase adsorbed layers reduce upon the addition of urea in the range of studied concentrations. The results agree with the theory that, upon unfolding, a distal region of the loop and tail domain forms adjacent to the proximal region of the interface. The exchange of matter between these regions reduces the viscoelasticity of the unfolded lipase adsorbed layers. Additionally, unfolding reduces the rigidity and brittleness of the lipase adsorbed layers: the aged adsorbed layer of native lipase can break upon high-amplitude perturbations of the interfacial area, unlike the case for urea-induced unfolded lipase.

Keywords: lipase; protein unfolding; interfacial dilational rheology; interfacial viscoelasticity; profile analysis tensiometer; urea-induced unfolding



Citation: Dowlati, S.; Javadi, A.; Miller, R.; Eckert, K.; Kraume, M. Unfolded Lipase at Interfaces Studied via Interfacial Dilational Rheology: The Impact of Urea. *Colloids Interfaces* **2022**, *6*, 56. <https://doi.org/10.3390/colloids6040056>

Academic Editor: Younjin Min

Received: 31 August 2022

Accepted: 10 October 2022

Published: 17 October 2022

Publisher's Note: MDPI stays neutral with regard to jurisdictional claims in published maps and institutional affiliations.



Copyright: © 2022 by the authors. Licensee MDPI, Basel, Switzerland. This article is an open access article distributed under the terms and conditions of the Creative Commons Attribution (CC BY) license (<https://creativecommons.org/licenses/by/4.0/>).

1. Introduction

Lipase is an enzyme that catalyzes triglyceride cleavage [1]. Triglycerides, the most common type of lipids, are composed of three fatty acids attached to a glycerol backbone by ester bonds. Lipase can break these bonds one by one and produces diglyceride, monoglyceride, and glycerol, respectively, as well as three free fatty acids [2]. Lipase is a hydrophilic molecule, while its primary substrate, triglyceride, is hydrophobic. So, the enzymatic reaction of lipid splitting occurs at the triglyceride–water interface as heterogeneous catalysis [2]. Further, lipase activates enzymatically upon adsorption to the interface, which leads to a subtle conformational change and opening of the active site [3]. Therefore, understanding lipase interfacial behavior is essential to optimize the kinetics of enzymatic catalysis of triglycerides.

Lipase unfolding can interrupt its enzymatic activity. Different agents can contribute to the unfolding of lipase, including temperature, pH, and denaturants. Unfolding is accompanied by the loss of stability and rigidity of protein structure upon breaking intraprotein bonds from the weakest to the strongest ones, respectively [4]. Urea, CO(NH₂)₂,

is a chaotropic agent that disrupts the hydrogen-bonding pattern of native proteins. Urea mainly changes the secondary structure of proteins by preferentially influencing the β -sheets more than α -helices [5]. The urea impact on the unfolding of different proteins has been frequently addressed, e.g., for β -lactoglobulin [6–9], lysozyme [10], bovine serum albumin [9,11], and human serum albumin [12].

Spectroscopic analysis has shown lipase structural unfolding in the presence of urea [13]. Urea-induced unfolding in the lipase native structure can result in amyloid fibril formation, in which proteins aggregate in a continuous β -sheet structure [14,15]. Molecular dynamics demonstrated that urea destabilizes the β -lactoglobulin structure by breaking the hydrogen bonds and also weakening the protein–protein hydrophobic interactions [16]. The dynamic interfacial elasticity and interfacial tension of lysozyme adsorbed layers decrease by increasing urea concentration, resulting in the lysozyme's molten globule state at the interface [10,17]. The molten globule is a compact, intermediate state between the native and unfolded states of a globular protein, in which the tertiary structure of the protein has deteriorated while the secondary structure is preserved [18].

The interfacial viscoelasticity of protein adsorbed layers plays a crucial role in stabilizing emulsions and foams [19]. Due to their intermolecular networking, protein adsorbed layers are strongly cohesive and stable towards external mechanical perturbations [9]. Interfacial dilational rheology is a technique that explores the dynamic viscoelasticity of the adsorbed layers by imposing mechanical deformations on the interfacial area. This technique has shown a promising application in providing invaluable information on the interfacial morphology and packing of molecules at the adsorbed layer [20,21]. Dynamic tensiometry combined with interfacial dilational rheology has been frequently applied to investigate the morphology of mixed layers in the presence of lipase [3,22–25].

The interfacial dilational rheology of globular and non-globular proteins can be distinguished by the evolution of the dynamic elasticity of the adsorbed layer [20]. For globular proteins, e.g., native lipase, the dynamic interfacial elasticity is higher and can monotonically increase over time or interfacial pressure, similar to charged nanoparticle adsorbed layers. For non-globular proteins, e.g., unfolded lipase, the dynamic interfacial elasticity shows local maximums similar to polymer solutions [10]. After these peaks, the interface switches to a thicker configuration, in which a dilute distal region of the tail and loop forms adjacent to the concentrated proximal region of the interface [26]. Protein chains can more readily exchange between these two regions than between the interface and bulk during interfacial perturbations. So, the viscoelasticity moduli can decrease owing to the more efficient interfacial relaxation processes [20].

In this study, we apply dynamic tensiometry and interfacial dilational rheology techniques to study the impact of lipase unfolding on the interfacial properties of the adsorbed layers. To this aim, urea is used as a strong denaturant. The effects of lipase and urea concentrations on the viscoelasticity of the adsorbed layers are investigated. Additionally, aging can change the configuration of adsorbed protein molecules, so its effect in the presence and absence of urea on the dilational rheology and lipase monolayer structure will be considered. At the triglyceride–water interface, the lipolysis products can change the composition of the adsorbed layer as a function of time, affecting the interfacial properties in ways similar to unfolding. Therefore, the impact of lipase unfolding is studied at the air–water interface to distinguish these two options. Previously, we have studied the interfacial dilational rheology of lipase layers at the oil–water interface [27].

2. Materials and Methods

2.1. Materials

The lipase, LipomodTM 34P-L034P, from *Candida rugosa* was provided by Biocatalysts Ltd. (Cardiff, UK), having an activity of 115,000 U·g^{−1}. Urea (GR for analysis ACS, Reag. Ph Eur) with purity ≥ 99.5 mol% determined by differential scanning calorimetry was purchased from Merck KGaA (Darmstadt, Germany). The urea solution of 5 molal has an initial IFT of ~ 74.5 mN·m^{−1} at the water–air interface but slightly decreases over time,

probably due to the smallest amounts of impurity. The urea solutions show no considerable interfacial viscoelasticity.

Lipase solution was prepared by adding dry powder of LIPOMOD™ 34P-L034P to deionized water or urea solutions while mildly stirred for 60 min and then ultrasonicated for 10 min. The concentration of lipase solutions in all cases is reported with respect to the deionized water volume, excluding urea's impact on the solution volume. The studied urea solutions of 0.1, 1.0, 2.0, and 5.0 molal correspond to 0.6, 5.7, 10.7, and 23.1 Wt. % or 0.1, 0.95, 1.8, and 4.1 M, respectively. All solutions were tested freshly after preparation. All aqueous solutions were prepared with deionized water prepared by PURELAB® Flex (Veolia Water Solutions & Technologies, High Wycombe, UK), having a conductivity of 0.055 μS . All interfacial tension and viscoelasticity experiments were performed at a room temperature of 24 °C. All measurements have been carried out after calibration of the setup by measuring the surface tension of water to obtain $\sim 72.0 \text{ mN}\cdot\text{m}^{-1}$ at 24 °C. Some errors in the range of $\pm 0.2 \text{ mN}\cdot\text{m}^{-1}$ are inevitable due to ambient conditions changes. After proper calibration, the accuracy in measuring the IFT is limited only to the setup resolution, $\pm 0.1 \text{ mN}\cdot\text{m}^{-1}$.

2.2. Interfacial Dilational Rheology

The profile analysis tensiometer (PAT) is based on axisymmetric drop shape analysis designed and manufactured by SINTERFACE Technologies e.K. (Berlin, Germany). The PAT protocol consists of capturing images of droplet shapes and digitizing the droplet profiles. Then, the digitized profiles are fitted by the Young–Laplace equation by adjusting the interfacial tension as the fitting parameter. The parametric form of the Young–Laplace equation is as follows [28]:

$$\frac{dx}{ds} = \cos \theta \quad (1)$$

$$\frac{dz}{ds} = \sin \theta \quad (2)$$

$$\frac{d\theta}{ds} = \frac{2}{R_0} - \frac{\Delta\rho \cdot g \cdot z}{\gamma} - \frac{\sin \theta}{x} \quad (3)$$

In the x - z coordinate system, R_0 is the radius of curvature at the apex of the droplet, γ is the interfacial tension, $\Delta\rho$ is the density difference between the droplet and the surrounding phase, s is the arc length of the droplet profile from the apex, and θ is the angle between the tangent line to the droplet and the horizon. The schematic representation of the PAT setup is shown in Figure 1.

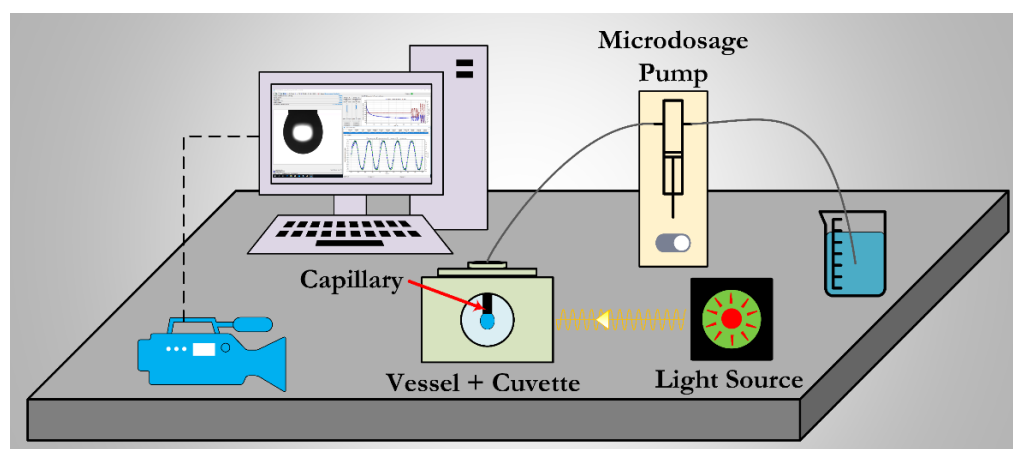


Figure 1. Schematic representation of a profile analysis tensiometer (reproduced with permission from [24], Copyright 2020 American Chemical Society).

Interfacial dilational rheology is a technique to investigate the viscoelasticity of interfacial layers by imposing area perturbations on the droplet surface and measuring its IFT response. For the straightforward analysis, area perturbations are usually conducted in sinusoidal harmonic forms [29]:

$$A(t) - A_0 = \Delta A(t) = A_{amp} \cdot \sin(\omega t) \quad (4)$$

$$\gamma(t) - \gamma_0 = \Delta \gamma(t) = \gamma_{amp} \cdot \sin(\omega t + \varphi) \quad (5)$$

Here, A is the interfacial area, γ is the interfacial tension, A_0 and γ_0 are the equilibrium, non-oscillating area and interfacial tension, A_{amp} and γ_{amp} are the corresponding amplitudes, ω is the angular frequency, t is time, and φ is the phase shift. The complex viscoelasticity, $\varepsilon(i\omega)$, is a transfer function that relates the area perturbations and their corresponding IFT responses in the frequency domain:

$$\varepsilon(i\omega) = \frac{\mathcal{F}[\Delta\gamma(t)]}{\mathcal{F}[\ln(\Delta A(t))]} \cong A_0 \frac{\mathcal{F}[\Delta\gamma(t)]}{\mathcal{F}[\Delta A(t)]} \quad (6)$$

$$\varepsilon(i\omega) = \varepsilon'(\omega) + i \cdot \varepsilon''(\omega) = \varepsilon_d(\omega) + i \cdot \omega \cdot \eta_d(\omega) \quad (7)$$

\mathcal{F} is the Fourier transform operator, ε' and ε'' are the real and imaginary components of the complex viscoelasticity, ε_d is the dilational modulus of elasticity, and η_d is the dilational modulus of viscosity [30,31].

3. Results and Discussion

3.1. Effect of Urea Concentration on Viscoelasticity of Lipase Adsorbed Layers

By increasing urea concentration, stepwise destruction of lipase structure is expected. The effect of urea concentration on the dynamic interfacial tensions of adsorbed layers from $2 \text{ mg} \cdot \text{mL}^{-1}$ lipase solution is shown in Figure 2a. Additionally, a set of sinusoidal perturbations with the same frequency and different amplitudes were imposed on the adsorbed layers to explore their viscoelastic properties. Increasing the urea concentration leads to a decrease in the interfacial tension of the adsorbed layers. Regarding the denaturing effect of urea, the reduction in IFT results from the unfolding of lipase. Unfolding increases the molar area of protein at the interface, enhancing the penetration of the protein segments into the interface and reducing the IFT.

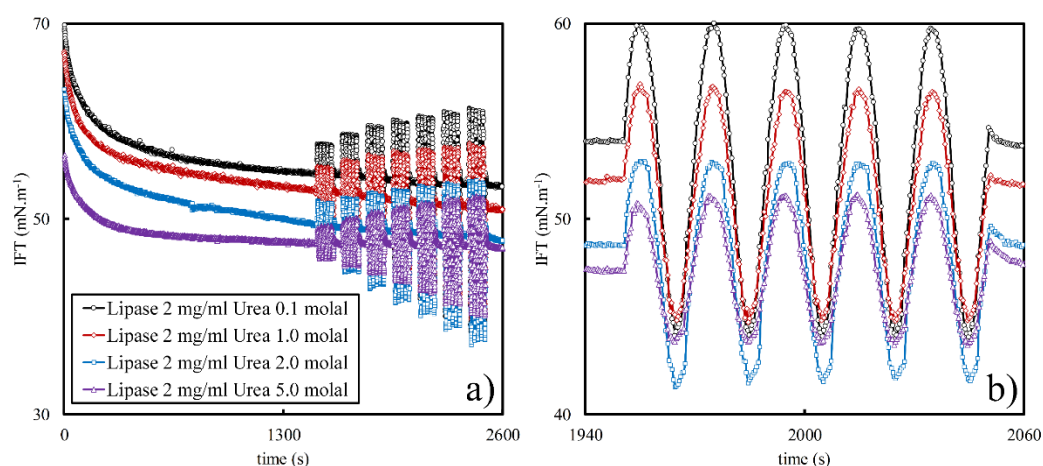


Figure 2. (a) Effect of urea on the dynamic interfacial tensions of the adsorbed layers from lipase $2 \text{ mg} \cdot \text{mL}^{-1}$ solutions with urea concentrations of 0.1, 1.0, 2.0, and 5.0 molal while imposing area oscillations of different amplitudes; (b) zoomed-in view on one oscillation from (a) with the frequency of 0.05 Hz and the amplitude of 21% between 1950 and 2050 s; the solid lines are drawn as a guide for the eye.

The IFT responses of the lipase adsorbed layers during five periods of interfacial area oscillations between 1950 and 2050 s with a frequency of 0.05 Hz and amplitude of 21% ($\Delta A/A_0\%$) are zoomed into in Figure 2b. Increasing the urea concentration leads to smaller amplitudes of the IFT responses, which is a measure of the elasticity modulus. A similar study has shown that urea and guanidine hydrochloride solutions of 6 M reduce the IFT and elasticity of lysozyme adsorbed layers. Under the urea effect, the formation of molten globules for the lysozyme conformation is suggested [32]. Additionally, urea increases the interfacial pressure and decreases the elasticity of β -lactoglobulin and bovine serum albumin adsorbed layers. However, the urea impact can differ at dilute denaturant concentrations [9].

The viscoelastic moduli of the lipase adsorbed layers in the presence of different urea concentrations are shown in Figure 3. The data are plotted versus the amplitude and frequency of the interfacial oscillations to understand how the extent and rate of the mechanical deformations influence the interfacial properties of the adsorbed layers. This figure depicts that the addition of urea induces lipase unfolding, which, in turn, decreases the viscoelastic moduli of the adsorbed layers in the range of studied urea concentrations. Increasing the amplitude of deformations decreases the elasticity in the lower urea concentrations, i.e., 0.1, 1.0, and 2.0 molal. In contrast, at 5.0 molal urea concentration, the elasticity becomes slightly dependent on the amplitude, Figure 3a. The dependence of elasticity on the amplitude would mean that we are in the range of a non-linear IFT response. The complex viscoelasticity of the adsorbed layers in the linear region of IFT response is only a function of frequency, i.e., $\varepsilon = \varepsilon(i\omega)$ [33].

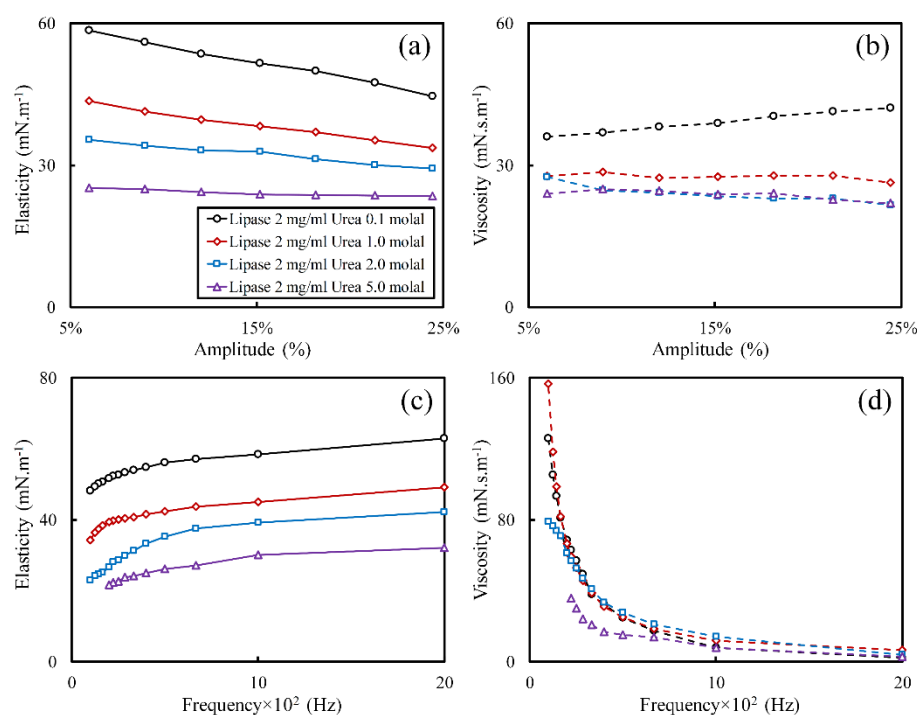


Figure 3. Effect of urea on the interfacial viscoelastic properties of the adsorbed layers from lipase $2.0 \text{ mg}\cdot\text{mL}^{-1}$ solutions with urea concentrations of 0.1, 1.0, 2.0, and 5.0 molal: effect of amplitude (a,b) and frequency (c,d) of the imposed sinusoidal perturbations of the interfacial area on the elasticity and viscosity of the adsorbed layers; the solid and dashed lines are drawn as a guide for the eye.

Additionally, viscosity increases with the amplitude at 0.1 molal urea concentration, while their dependency decreases by increasing urea concentration, Figure 3b. As a result, the unfolding leads to a more linear IFT response of the interfacial adsorbed layer in the range of study. This effect can result from the distal region formation, providing a more efficient exchange of protein tails and loops between the distal and proximal regions upon the mechanical deformations of the interface.

The dependency of the viscoelastic moduli on the frequency is shown in Figure 3c,d. Increasing the frequency increases the elasticity owing to the shorter time provided for the adsorbed layer to reach its equilibrium state. Additionally, the viscosity decreases when we generate faster oscillations of the interface, suggesting smaller delays in the IFT responses. We will see the same effect for all lipase adsorbed layers investigated in this study. Again, adding urea gives rise to lower values of the viscoelastic moduli versus frequency since protein loses its globular structure resulting from the breakage of the intra-protein bonds, e.g., disulfide bridges and hydrogen bonds.

As long as the IFT response of an adsorbed layer is in a pure sinusoidal form, such as in Equation (5), the IFT response can be in the region of linearity, provided that γ_{amp}/A_{amp} remains constant to keep the viscoelasticity independent of amplitude. Accordingly, the time parameter can be eliminated between Equations (4) and (5) [27]:

$$A_D^2 + \gamma_D^2 - 2\cos(\varphi) \cdot A_D \cdot \gamma_D = \sin^2(\varphi) \quad (8)$$

where $A_D = (A(t) - A_0)/A_{amp}$ and $\gamma_D = (\gamma(t) - \gamma_0)/\gamma_{amp}$ are the dimensionless interfacial area and dimensionless IFT, and φ is the phase shift of the IFT response. Equation (8) demonstrates the Lissajous plot (dimensionless interfacial tension vs. dimensionless area) as an ellipse. Graphically, the slope of the ellipse's major axis is a measure of elasticity, and the length of the minor axis is a measure of viscosity. Under the inviscid condition, i.e., purely elastic, φ is zero, and Equation (8) becomes a line: $A_D = \gamma_D$. A non-linear IFT response of the adsorbed layer deforms the ellipsoid shape of the Lissajous plot in different ways, providing an opportunity for the qualitative analysis of the non-linearity extent.

The Lissajous plots for the lipase adsorbed layers at different urea concentrations and amplitudes of area oscillations are shown in Figure 4. At 0.1 molal urea concentration, the Lissajous plots are more inclined and more widely open than at higher urea concentrations. By increasing the amplitude, the plots deform towards non-ellipsoids, showing an increase in the extent of non-linearity of the IFT response, as expected. By increasing the urea concentration, the plots become narrower and less inclined. Hydrogen bonds and disulfide bridges highly interconnect globular proteins. Breaking these bonds by adding urea leads to molten globules or even disordered structures, making the interface more flexible during deformations.

3.2. Effect of Urea on Viscoelasticity of Droplet Surfaces

This section explores the viscoelasticity of aqueous urea solutions without lipase to determine its role in the viscoelasticity of the mixed adsorbed layers. The interfacial tensions of aqueous solutions of 1.0, 2.0, and 5.0 molal urea are shown in Figure 5a. By increasing the urea concentration, the initial IFT increases, similar to brine solutions, by having an interfacial concentration less than the bulk concentration [34]. However, the dynamic IFT shows a slight downward trend, probably because of impurities in the urea sample.

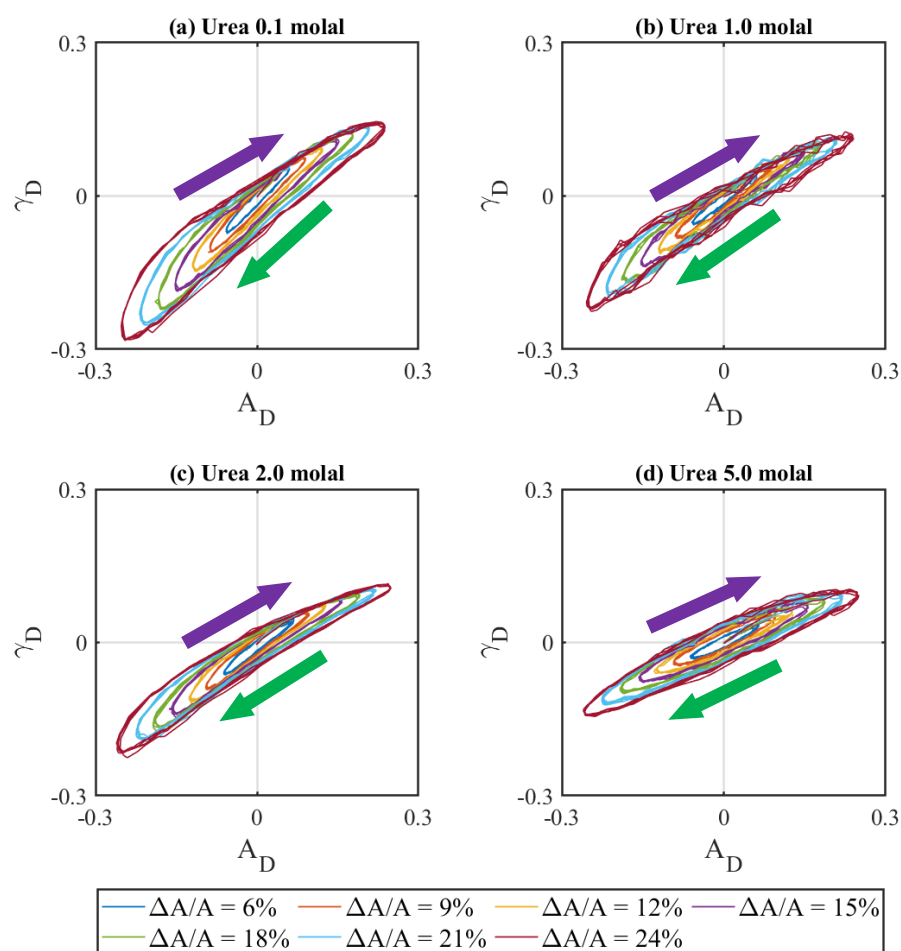


Figure 4. Effect of urea on the Lissajous plot of the adsorbed layers from lipase $2 \text{ mg} \cdot \text{mL}^{-1}$ solution with urea concentrations of 0.1, 1.0, 2.0, and 5.0 molal by oscillations of 0.05 Hz frequency and different amplitudes; the compression and expansion paths are denoted with green and purple arrows, respectively; $\Delta A / A$ for Lissajous plots from inside towards outside are 6% (blue), 9% (orange), 12% (yellow), 15% (purple), 18% (green), 21% (light blue), and 24% (red), respectively; solid lines are used for better visualization of experimental results.

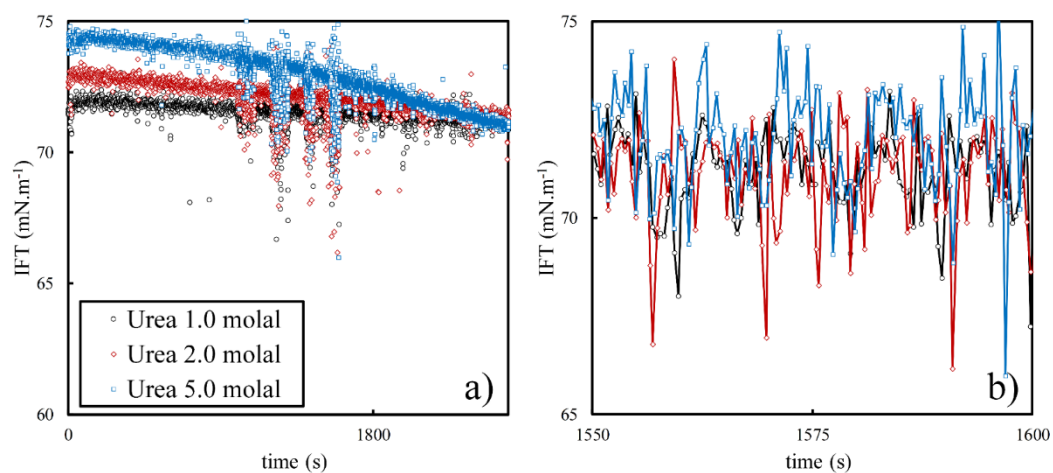


Figure 5. (a) Interfacial tension of urea solutions of 1.0, 2.0, and 5.0 molal while imposing area oscillations of different amplitudes; (b) zoomed-in view on one oscillation from (a) with the frequency of 0.1 Hz and the amplitude of 17%; the solid lines are drawn as a guide for the eye.

The IFT responses of the urea solutions to the area oscillations of 0.1 Hz frequency and 17% amplitude between 1550 and 1600 s are shown in Figure 5b. The key point is that the IFT responses are highly scattered, not showing a sinusoidal trend. This behavior indicates a lack of interfacial layers, leading to a non-viscoelastic interfacial behavior. However, the sinusoidal regression may be misleading in such cases by providing high values for the viscoelastic moduli while the fitting quality is poor. The total harmonic distortion (*THD*) is a parameter that can describe the quality of fitting sinusoids to the IFT response:

$$THD = \frac{(a_2^2 + a_3^2 + \dots + a_n^2)^{1/2}}{a_1} \quad (9)$$

where a_1 is the amplitude of the fundamental frequency (ω) after imposing a Fourier transform on the IFT response, and the a_i 's ($i = 2, \dots, n$) are amplitudes of the higher harmonics, namely $2\omega, 3\omega, \dots, n\omega$ [33].

For the viscoelastic adsorbed layers, the *THD* determines the degree of non-linearity of the IFT response. A *THD* value of more than 5% indicates non-linearity. In addition, for non-viscoelastic adsorbed layers, *THD* determines the signal-to-noise ratio of the IFT response. While for lipase adsorbed layers with or without urea, the *THD* exceeds 10% only for high-amplitude oscillations, the *THD* of urea solutions can exceed 100%, indicating that a viscoelastic layer is not formed.

3.3. Effect of Interface Age

It is long believed that proteins unfold at interfaces upon adsorption; however, the extent of unfolding is highly controversial [20]. The characteristics of a protein adsorbed layer can evolve by aging due to the change in the adsorption state, protein structure, and adsorbed concentration. Additionally, interfacial interprotein networking can influence the interfacial properties over time, suggesting that the interface age is a determining parameter. In practice, lipase-catalyzed reactions are not fast: the enzymatic catalysis of triglycerides using free lipase can reach an ultimate yield in six hours, after which the conversion curve levels off [35]. So, the effect of aging on lipase interfacial conformation during the effective reaction time is a matter of concern.

The IFT of $2 \text{ mg}\cdot\text{mL}^{-1}$ lipase solutions with and without urea for 6 h is shown in Figure 6. Similar interfacial oscillations were applied every 30 min during the first five hours. After that, the frequency and amplitudes of the oscillations were varied. The IFT does not equilibrate during both tests, showing that the interfacial concentration and structure change dynamically. The IFT of lipase solutions in the presence of urea remains lower than for pure lipase, suggesting the destruction of the lipase globules and exposing more protein segments to the interface.

Increasing the amplitude of oscillations for $2 \text{ mg}\cdot\text{mL}^{-1}$ lipase solutions increases the average IFT between 5.2 and 5.6 h (highlighted by a gray background in Figure 6). This phenomenon can result from a lipase monolayer breakage caused by high-amplitude oscillations. By aging, the adsorbed layer becomes more concentrated and more fully packed. Upon compression, the monolayer can buckle and then break. During expansion, if the multilayer aggregates cannot reestablish their monolayer structure, they stay as separate islands, and the fresh interface between them will be ready for more adsorption. A similar effect has been observed for polymerized styrene microparticles [36] and complexes of silica nanoparticles with CTAB [37]. Meanwhile, urea-induced unfolding reduces the chance of monolayer breakage owing to the deterioration of the globular structure of lipase molecules and the formation of loops and tails, facilitating matter exchange between the proximal and distal regions. Upon unfolding, the rigidity of the protein structure reduces, becoming more flexible by losing some of its hydrogen bonds.

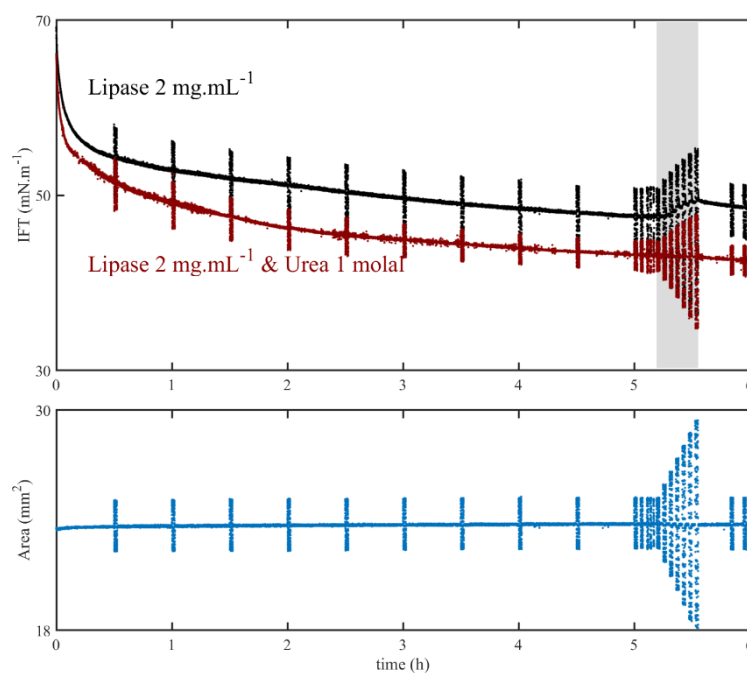


Figure 6. Effect of aging on the dynamic interfacial tension of the adsorbed layers from 2 mg.mL⁻¹ lipase solutions without and with 1 mola urea (**top**) and the imposed oscillations on the droplet area (**bottom**); the period of amplitude sweep is shown with a gray background.

The interfacial dilational viscoelasticity of the adsorbed layers from 2 mg.mL⁻¹ lipase solutions in the presence and absence of urea over six hours is shown in Figure 7a. In the presence of urea, the viscoelastic moduli are lower. Additionally, the elasticity values level off with time after a decrease, and the viscosity shows an overall decreasing trend. The reduction in IFT owing to more adsorption can lead to lower viscoelastic properties. Previous studies have shown that the elasticity modulus of unfolded proteins shows one or two local maximums with increasing interfacial pressure [20]. By comparison, this study is in the concentration range of inverse proportionality between elasticity and interfacial pressure. The last two points of the pure adsorbed layer of lipase are recorded after the breakage of the monolayer by high-amplitude perturbations of the interface, showing a great contrast with other points. In the presence of urea, a similar effect is not observed.

The frequency effect on the aged adsorbed layers of lipase is shown in Figure 7b. Viscosity shows more sensitivity to the frequency than elasticity and decreases vs. frequency. The effect of amplitude on the viscoelasticity in the presence of urea is small, Figure 7c, indicating that unfolding renders the IFT response of a lipase adsorbed layer more linearly. Without urea, the elasticity decreases, and the viscosity first increases and then decreases with the increasing amplitude of the oscillations.

The study of an amplitude sweep (varying amplitude at a constant frequency) is usually conducted outside of the linear viscoelastic regime of the adsorbed layer to explore its mechanical properties similar to the actual processes in nature or industry [38]. The Lissajous plot gives us insight into the extent of the non-linearity. The Lissajous plots for the aged lipase layers during high-amplitude interfacial perturbations are shown in Figure 8. In the presence of urea, the Lissajous plots become more ellipsoidal with less inclination and smaller openings, indicating decreases in the viscoelastic moduli. Additionally, for pure lipase, the difference between the compression and expansion slopes of the plots becomes more notable, suggesting a shift in the interfacial regime consistent with the phenomenon of breakage of the adsorbed layer.

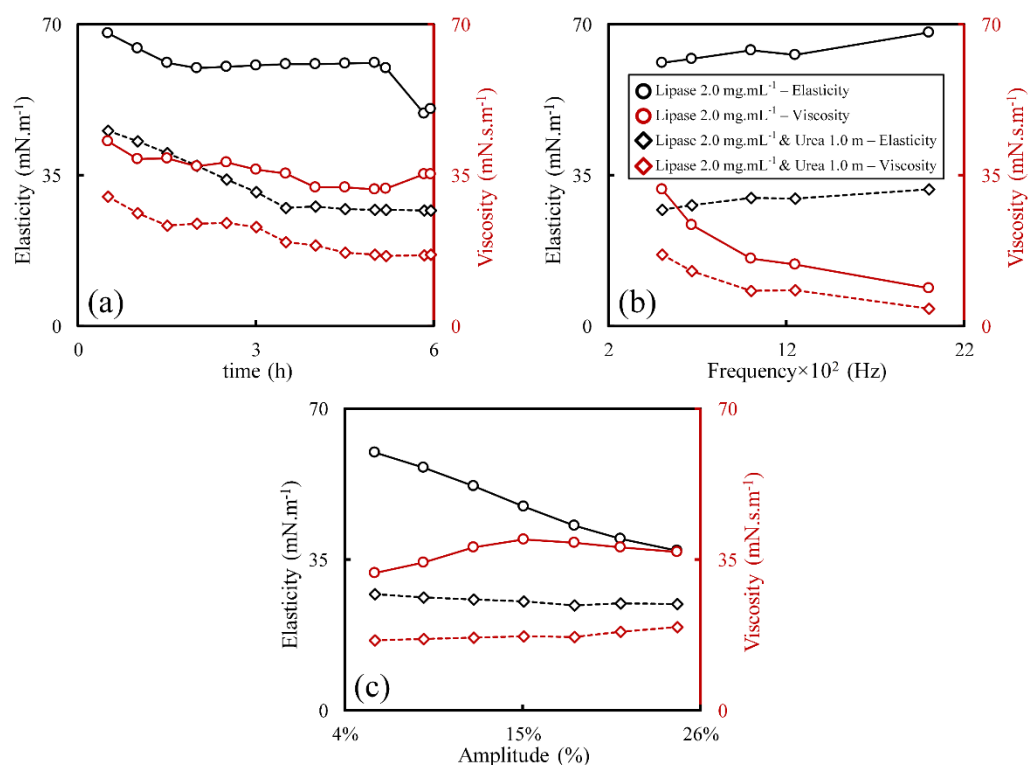


Figure 7. Effect of aging on the viscoelastic properties of the adsorbed layers from 2 mg.mL⁻¹ lipase solution in the absence and presence of 1 molal urea: (a) viscoelasticity evolution over time studied by imposing sinusoidal perturbations of 0.05 Hz frequency and 5% amplitude ($\Delta A/A_0$); (b) viscoelasticity versus frequency studied after 18,000 s from the start of the test; (c) viscoelasticity versus amplitude studied after 18,700 s from the beginning of the test; the solid and dashed lines are drawn as guides for the eye.

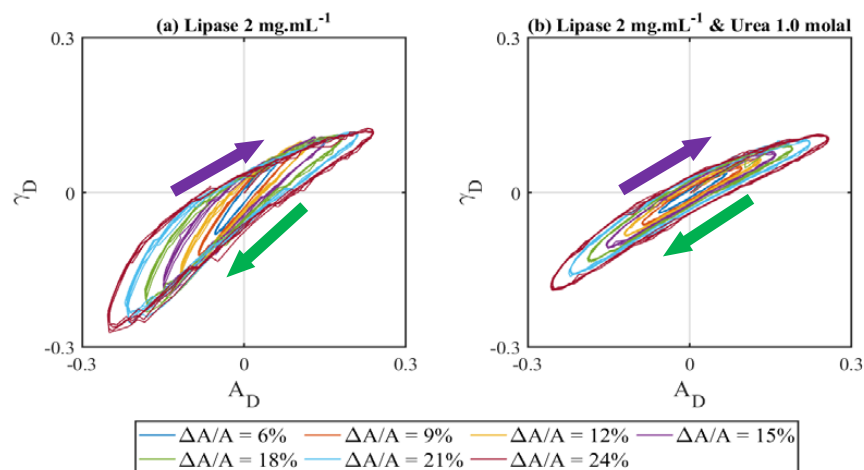


Figure 8. The effect of amplitude sweep on the Lissajous plot of aged adsorbed layers for 5.2 h of 2 mg.mL⁻¹ lipase solutions without and with 1 molal urea; the compression and expansion paths are denoted with green and purple arrows, respectively; $\Delta A/A$ for Lissajous plots from inside towards outside are 6% (blue), 9% (orange), 12% (yellow), 15% (purple), 18% (green), 21% (light blue), and 24% (red), respectively; solid lines are used for better visualization of experimental results.

Different mechanisms can be suggested for the compressive behavior of the native and unfolded lipase adsorbed layers after aging. The globular shape of the lipase native structure, its rigidity, and the undisturbed pattern of protein–protein interactions result in the brittleness of the aged adsorbed layer of lipase. On the other hand, the adsorbed layer of

unfolded lipase is more flexible due to the more unstructured conformation of proteins. So, for native lipase, the adsorbed layer can break upon the compression of the interface, giving rise to a multilayer structure of the adsorbed proteins. Upon expansion, these multilayers cannot retrieve their monolayer structure, remaining as multilayer islands, while the freshly generated interface is yet unoccupied. This phenomenon causes higher IFTs and lower elasticities. Meanwhile, the less rigid structures of unfolded lipase act as flexible entities, making the adsorbed layer more stable towards compression forces. A schematic of the suggested mechanisms is shown in Figure 9.

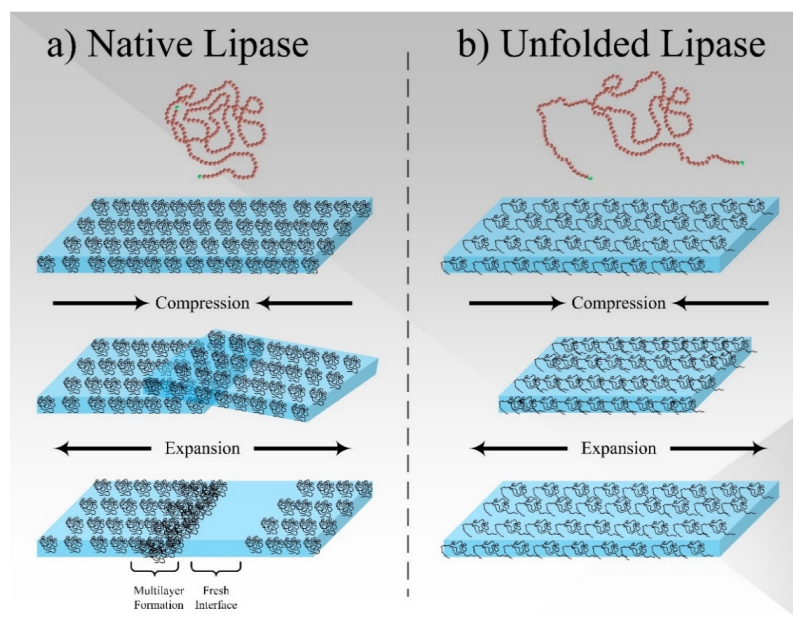


Figure 9. Schematic representation of the suggested mechanism for the high-amplitude compression deformation of the native and unfolded lipase adsorbed layers after aging.

3.4. Effect of Lipase Concentration

The bulk concentration determines interfacial concentration based on the corresponding adsorption isotherm. The study of the urea effect on the lipase structure at different concentrations is summarized in Figure 10. Lipase at concentrations of 0.5, 1.0, 3.0, and 5.0 mg·mL⁻¹ was investigated in the absence and presence of 1 molal urea. The key results are similar to the previous tests: urea reduces the IFT, elasticity, and viscosity of lipase adsorbed layers. Over time, the gap between the IFT of lipase with and without urea becomes wider (the IFT with urea decreases faster). Unfolded lipase has more contact points with the interface than globular lipase, which leads to higher interfacial pressures at the same interfacial concentration. The concentration does not show a uniform impact on the viscoelastic moduli. At early times, the 0.5 mg·mL⁻¹ lipase solution has elasticities lower than 1.0 mg·mL⁻¹ lipase compared to the late times since the interfacial network is not sufficiently developed at early times and low concentrations. At the studied concentrations, the elasticity decreases with concentration. The effect of the amplitude on the viscoelastic moduli (Figure 10(a4,a5,b4,b5)) are recorded similarly to Figure 2—the corresponding IFT plots are not shown here. Urea reduces the differences between different lipase concentrations and makes the IFT response of the adsorbed layers more linear.

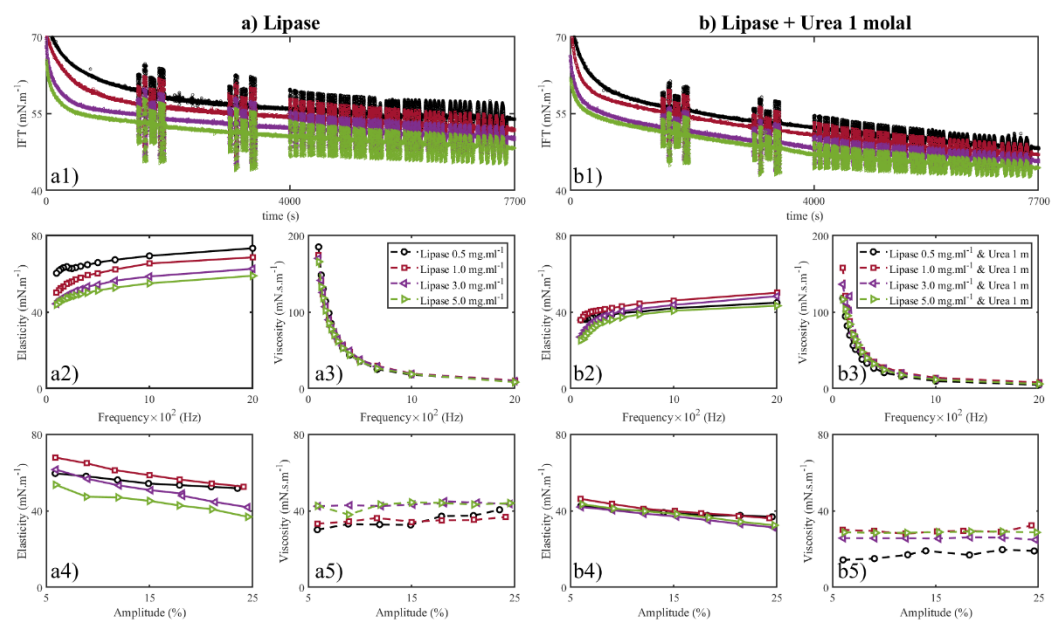


Figure 10. Effect of lipase concentration on the interfacial tension and viscoelasticity of the adsorbed layer at the air–water interfaces: (a) pure lipase and (b) lipase and 1 molal urea mixtures; (a1) dynamic interfacial tension of adsorbed layers from lipase solutions of 0.5, 1.0, 3.0, 5.0 mg·mL^{−1} over time; (b1) dynamic interfacial tension of adsorbed layers from lipase solutions of 0.5, 1.0, 3.0, 5.0 mg·mL^{−1} and urea 1 molal over time; (a2,a3,b2,b3) effect of the interfacial oscillation frequency on the viscoelastic moduli of the interface; (a4,a5,b4,b5) effect of the interfacial oscillation amplitude on the viscoelastic moduli of the interface; the solid and dashed lines are drawn as a guide for the eye.

4. Conclusions

Our results show that urea leads to the unfolding of the lipase molecules in the range of the studied concentrations by destroying its globular structure. This unfolding decreases the equilibrium IFT and viscoelastic moduli of the adsorbed layers. The results are in accordance with the theory of loop and tail formation: upon unfolding, a diluted distal region of loops and tails of the lipase molecules is formed adjacent to the concentrated proximal region of the interface. This transition brings about a thicker interfacial region. The corresponding exchange of lipase segments between the distal and proximal regions gives rise to smaller viscoelastic moduli of the adsorbed layer.

The urea-induced unfolding of lipase makes the IFT response of the adsorbed layers more linear by reducing the dependency of the interfacial viscoelasticity on the amplitude of sinusoidal area perturbations. This effect can be regarded as a measure of the unfolding of globular proteins and can be qualitatively analyzed using Lissajous plots.

The globular structure of native lipase shows a behavior similar to particle-laden adsorbed layers: its monolayer can break upon aging. This phenomenon can be detected by increasing the average IFT of the aged lipase adsorbed layer due to high-amplitude oscillations. After the breakage of the monolayer upon compression, its primary morphology cannot be retrieved by expansion, and separate multilayer islands lead to higher IFT and lower elasticity.

Our results show the promising application of dilational rheology to study the unfolding of lipase and its effect on the interfacial properties of interfacial layers. Furthermore, the same approach can be applied to study the impact of other unfolding protocols, e.g., temperature, pH, alcohols, electrolytes, and surfactants, on the adsorbed layers of lipase and other proteins.

Author Contributions: Conceptualization, S.D.; methodology, S.D., A.J. and R.M.; validation, S.D., A.J., R.M., K.E. and M.K.; formal analysis, S.D. and R.M.; investigation, S.D.; resources, S.D., K.E. and M.K.; data curation, S.D.; writing—original draft preparation, S.D.; writing—review and editing,

S.D. and R.M.; visualization, S.D.; supervision, K.E. and M.K.; project administration, M.K.; funding acquisition, M.K. All authors have read and agreed to the published version of the manuscript.

Funding: This research is funded by the German Research Foundation (DFG)-TRR 63 “Integrated Chemical Processes in Liquid Multiphase Systems” (subproject Z1)–56091768 (Gefördert durch die Deutsche Forschungsgemeinschaft (DFG)-TRR 63 “Integrierte chemische Prozesse in flüssigen Mehrphasensystemen” (Teilprojekt Z1)–56091768).

Data Availability Statement: Not applicable.

Conflicts of Interest: The authors declare no conflict of interest. The funders had no role in the design of the study, in the collection, analyses, or interpretation of data, in the writing of the manuscript, or in the decision to publish the results.

References

1. Svendsen, A. Lipase protein engineering. *Biochim. Biophys. Acta (BBA) Protein Struct. Mol. Enzymol.* **2000**, *1543*, 223–238. [[CrossRef](#)]
2. Freedman, B.; Butterfield, R.O.; Pryde, E.H. Transesterification kinetics of soybean oil 1. *J. Am. Oil Chem. Soc.* **1986**, *63*, 1375–1380. [[CrossRef](#)]
3. Reis, P.; Holmberg, K.; Watzke, H.; Leser, M.E.; Miller, R. Lipases at interfaces: A review. *Adv. Colloid Interface Sci.* **2009**, *147*, 237–250. [[CrossRef](#)]
4. Rader, A.J.; Hespeneheide, B.M.; Kuhn, L.A.; Thorpe, M.F. Protein unfolding: Rigidity lost. *Proc. Natl. Acad. Sci. USA* **2002**, *99*, 3540–3545. [[CrossRef](#)] [[PubMed](#)]
5. Rocco, A.G.; Mollica, L.; Ricchiuto, P.; Baptista, A.M.; Gianazza, E.; Eberini, I. Characterization of the Protein Unfolding Processes Induced by Urea and Temperature. *Biophys. J.* **2008**, *94*, 2241–2251. [[CrossRef](#)] [[PubMed](#)]
6. Busti, P.A.; Scarpeci, S.; Gatti, C.; Delorenzi, N. Use of fluorescence methods to monitor unfolding transitions in β -lactoglobulin. *Food Res. Int.* **2002**, *35*, 871–877. [[CrossRef](#)]
7. Czarnik-Matuszewicz, B.; Bin Kim, S.; Jung, Y.M. A Study of Urea-dependent Denaturation of β -Lactoglobulin by Principal Component Analysis and Two-dimensional Correlation Spectroscopy. *J. Phys. Chem. B* **2008**, *113*, 559–566. [[CrossRef](#)]
8. D’Alfonso, L.; Collini, M.; Baldini, G. Does β -Lactoglobulin Denaturation Occur via an Intermediate State? *Biochemistry* **2002**, *41*, 326–333. [[CrossRef](#)]
9. Mikhailovskaya, A.; Noskov, B.; Nikitin, E.; Lin, S.-Y.; Loglio, G.; Miller, R. Dilational surface viscoelasticity of protein solutions. Impact of urea. *Food Hydrocoll.* **2014**, *34*, 98–103. [[CrossRef](#)]
10. Tihonov, M.M.; Milyaeva, O.Y.; Noskov, B.A. Dynamic surface properties of lysozyme solutions. Impact of urea and guanidine hydrochloride. *Colloids Surf. B Biointerfaces* **2015**, *129*, 114–120. [[CrossRef](#)]
11. Das, A.; Chitra, R.; Choudhury, R.R.; Ramanadham, M. Structural changes during the unfolding of Bovine serum albumin in the presence of urea: A small-angle neutron scattering study. *Pramana* **2004**, *63*, 363–368. [[CrossRef](#)]
12. Leggio, C.; Galantini, L.; Konarev, P.V.; Pavel, N.V. Urea-Induced Denaturation Process on Defatted Human Serum Albumin and in the Presence of Palmitic Acid. *J. Phys. Chem. B* **2009**, *113*, 12590–12602. [[CrossRef](#)] [[PubMed](#)]
13. Chaitanya, P.K.; Prabhu, N.P. Stability and Activity of Porcine Lipase Against Temperature and Chemical Denaturants. *Appl. Biochem. Biotechnol.* **2014**, *174*, 2711–2724. [[CrossRef](#)] [[PubMed](#)]
14. Rashno, F.; Khajeh, K.; Capitini, C.; Sajedi, R.H.; Shokri, M.M.; Chiti, F. Very rapid amyloid fibril formation by a bacterial lipase in the absence of a detectable lag phase. *Biochim. Biophys. Acta (BBA) Proteins Proteom.* **2017**, *1865*, 652–663. [[CrossRef](#)] [[PubMed](#)]
15. Qafary, M.; Khajeh, K.; Ramazzotti, M.; Moosavi-Movahedi, A.A.; Chiti, F. Urea titration of a lipase from *Pseudomonas* sp. reveals four different conformational states, with a stable partially folded state explaining its high aggregation propensity. *Int. J. Biol. Macromol.* **2021**, *174*, 32–41. [[CrossRef](#)]
16. Eberini, I.; Emerson, A.; Sensi, C.; Ragona, L.; Ricchiuto, P.; Pedretti, A.; Gianazza, E.; Tramontano, A. Simulation of urea-induced protein unfolding: A lesson from bovine β -lactoglobulin. *J. Mol. Graph. Model.* **2011**, *30*, 24–30. [[CrossRef](#)]
17. Hédoux, A.; Krenzlin, S.; Paccou, L.; Guinet, Y.; Flament, M.-P.; Siepmann, J. Influence of urea and guanidine hydrochloride on lysozyme stability and thermal denaturation; a correlation between activity, protein dynamics and conformational changes. *Phys. Chem. Chem. Phys.* **2010**, *12*, 13189–13196. [[CrossRef](#)]
18. Kuwajima, K. The molten globule state as a clue for understanding the folding and cooperativity of globular-protein structure. *Proteins Struct. Funct. Bioinform.* **1989**, *6*, 87–103. [[CrossRef](#)]
19. Maldonado-Valderrama, J.; Martín-Rodríguez, A.; Gálvez-Ruiz, M.J.; Miller, R.; Langevin, D.; Cabrerizo-Vílchez, M.A. Foams and emulsions of β -casein examined by interfacial rheology. *Colloids Surf. A Physicochem. Eng. Asp.* **2008**, *323*, 116–122. [[CrossRef](#)]
20. Noskov, B.A. Protein conformational transitions at the liquid–gas interface as studied by dilational surface rheology. *Adv. Colloid Interface Sci.* **2014**, *206*, 222–238. [[CrossRef](#)]
21. Wang, N.; Zhang, Y.; Li, Y.; Liu, Y.; Wang, C.; Xu, B.; Zhao, L.; Xu, B. Interfacial rheological properties of cholesteryl-oligopeptide surfactants: Effects of hydrophilic group structure. *J. Mol. Liq.* **2022**, *365*, 120198. [[CrossRef](#)]
22. Wang, C.; Zhang, P.; Chen, Z.; Liu, Y.; Zhao, L.; Wang, N.; Xu, B. Effects of fatty acyl chains on the interfacial rheological behaviors of amino acid surfactants. *J. Mol. Liq.* **2021**, *325*, 114823. [[CrossRef](#)]

23. Reis, P.; Malmsten, M.; Nydén, M.; Folmer, B.; Holmberg, K. Interactions between lipases and amphiphiles at interfaces. *J. Surfactants Deterg.* **2019**, *22*, 1047–1058. [[CrossRef](#)]
24. Javadi, A.; Dowlati, S.; Miller, R.; Schneck, E.; Eckert, K.; Kraume, M. Dynamics of Competitive Adsorption of Lipase and Ionic Surfactants at the Water–Air Interface. *Langmuir* **2020**, *36*, 12010–12022. [[CrossRef](#)]
25. Mekkaoui, A.; Liu, Y.; Zhang, P.; Ullah, S.; Wang, C.; Xu, B. Effect of Bile Salts on the Interfacial Dilational Rheology of Lecithin in the Lipid Digestion Process. *J. Oleo Sci.* **2021**, *70*, 1069–1080. [[CrossRef](#)]
26. Noskov, B.A.; Mikhailovskaya, A.A.; Lin, S.-Y.; Loglio, G.; Miller, R. Bovine Serum Albumin Unfolding at the Air/Water Interface as Studied by Dilational Surface Rheology. *Langmuir* **2010**, *26*, 17225–17231. [[CrossRef](#)]
27. Javadi, A.; Dowlati, S.; Shourni, S.; Rusli, S.; Eckert, K.; Miller, R.; Kraume, M. Enzymatic Hydrolysis of Triglycerides at the Water–Oil Interface Studied via Interfacial Rheology Analysis of Lipase Adsorption Layers. *Langmuir* **2021**, *37*, 12919–12928. [[CrossRef](#)]
28. Hoorfar, M.; Neumann, A.W. Recent progress in Axisymmetric Drop Shape Analysis (ADSA). *Adv. Colloid Interface Sci.* **2006**, *121*, 25–49. [[CrossRef](#)]
29. Loglio, G.; Pandolfini, P.; Miller, R.; Makievski, A.V.; Krägel, J.; Ravera, F.; Noskov, B.A. Perturbation–response relationship in liquid interfacial systems: Non-linearity assessment by frequency–domain analysis. *Colloids Surfaces A Physicochem. Eng. Asp.* **2005**, *261*, 57–63. [[CrossRef](#)]
30. Loglio, G.; Tesei, U.; Cini, R. Dilational properties of monolayers at the oil-air interface. *J. Colloid Interface Sci.* **1984**, *100*, 393–396. [[CrossRef](#)]
31. Loglio, G.; Tesei, U.; Cini, R. Viscoelastic dilatation processes of fluid/fluid interfaces: Time-domain representation. *Colloid Polym. Sci.* **1986**, *264*, 712–718. [[CrossRef](#)]
32. Campbell, R.A.; Tummino, A.; Varga, I.; Milyaeva, O.Y.; Krycki, M.M.; Lin, S.-Y.; Laux, V.; Haertlein, M.; Forsyth, V.T.; Noskov, B.A. Adsorption of Denaturated Lysozyme at the Air–Water Interface: Structure and Morphology. *Langmuir* **2018**, *34*, 5020–5029. [[CrossRef](#)] [[PubMed](#)]
33. Bykov, A.; Liggieri, L.; Noskov, B.; Pandolfini, P.; Ravera, F.; Loglio, G. Surface dilational rheological properties in the nonlinear domain. *Adv. Colloid Interface Sci.* **2015**, *222*, 110–118. [[CrossRef](#)]
34. Sears, D.F. Surface activity of urea. *J. Colloid Interface Sci.* **1969**, *29*, 288–295. [[CrossRef](#)]
35. Rusli, S.; Grabowski, J.; Drews, A.; Kraume, M. A Multi-Scale Approach to Modeling the Interfacial Reaction Kinetics of Lipases with Emphasis on Enzyme Adsorption at Water–Oil Interfaces. *Processes* **2020**, *8*, 1082. [[CrossRef](#)]
36. Bykov, A.G.; Noskov, B.A.; Loglio, G.; Lyadinskaya, V.V.; Miller, R. Dilational surface elasticity of spread monolayers of polystyrene microparticles. *Soft Matter* **2014**, *10*, 6499–6505. [[CrossRef](#)]
37. Yazhgur, P.A.; Noskov, B.A.; Liggieri, L.; Lin, S.-Y.; Loglio, G.; Miller, R.; Ravera, F. Dynamic properties of mixed nanoparticle/surfactant adsorption layers. *Soft Matter* **2013**, *9*, 3305–3314. [[CrossRef](#)]
38. Hinderink, E.B.; Meinders, M.B.; Miller, R.; Sagis, L.; Schroën, K.; Berton-Carabin, C.C. Interfacial protein–protein displacement at fluid interfaces. *Adv. Colloid Interface Sci.* **2022**, *305*, 102691. [[CrossRef](#)]